Published in: Journal Of Non-Crystalline Solids (2011)
Status: Postprint (Author's version)

Preparation and characterization of ZnO-TiO_2 films obtained by sol-gel method

T. Ivanova [a], A. Harizanova [a], T. Koutzarova [b], B. Vertruyen[c]
[a] *Central Laboratory of Solar Energy and New Energy Sources, Bulgarian Academy of Sciences, blvd. Tzarigradsko chaussee 72, Sofia, Bulgaria*
[b] *Institute of Electronics, Bulgarian Academy of Sciences, blvd. Tzarigradsko chaussee 72, Sofia, Bulgaria*
[c] *LCIS/SUPRATECS, Institute of Chemistry B6, University of Liege, Sart-Tilman, B-4000 Liege, Belgium*

Abstract

The sol-gel route has been applied to obtain ZnO-TiO_2 thin films. For comparison, pure TiO_2 and ZnO films are also prepared from the corresponding solutions. The films are deposited by a spin-coated method on silicon and glass substrates. Their structural and vibrational properties have been studied as a function of the annealing temperatures (400-750 °C). Pure ZnO films crystallize in a wurtzite modification at a relatively low temperature of 400 °C, whereas the mixed oxide films show predominantly amorphous structure at this temperature. XRD analysis shows that by increasing the annealing temperatures, the sol-gel Zn/Ti oxide films reveal a certain degree of crystallization and their structures are found to be mixtures of wurtzite ZnO, Zn_2TiO_4, anatase TiO_2 and amorphous fraction. The XRD analysis presumes that Zn_2TiO_4 becomes a favored phase at the highest annealing temperature of 750 °C. The obtained thin films are uniform with no visual defects. The optical properties of ZnO-TiO_2 films have been compared with those of single component films (ZnO and TiO_2). The mixed oxide films present a high transparency with a slight decrease by increasing the annealing temperature.

Keywords*:* Metal oxides films; Sol-gel technology; X-Ray diffraction; Optical properties

1. INTRODUCTION

Recently, zinc oxide has attracted scientific research as a particularly interesting material due to its unique properties such as high chemical stability, good electrical properties, high luminous transmittance, excellent substrate adherence, hardness, optical and piezoelectric behavior and low price [1]. Possible and proven applications include light emitting diodes [2], photodetectors [3], gas sensors [4], dye sensitized solar cells (DSSC) [5] etc. Furthermore, ZnO is a promising material for usage in short wavelength light emitting devices and daylight-blind UV detectors [6].

Titanium oxide is also a well-known semiconductor and it has been shown as one of the most important materials for application as a gas sensor [7]and an antireflective coating [8]. TiO_2 is used in electrochromic devices and solar cells [9]. The high photocatalytic properties and photosensitivity of TiO_2 have been intensively studied [10].

Thin films of TiO_2 and ZnO can be deposited by a variety of physical and chemical technologies such as magnetron sputtering, CVD and electrochemical method [11-13]. The Sol-gel route is a wet-chemical deposition suitable for fabrication of thin films, ceramics, fibers and nanocomposites [14,15]. This approach possesses several advantages including homogeneity and uniformity of the obtained films, easy control of composition, possibility of preparing metal oxide mixtures in a predictable way, large area depositions, cost effectiveness, etc. [16].

ZnO-TiO_2 nanostructured systems have shown many applications as gas sensing materials [17], antistatic films, catalysts [18,19] and antireflective coatings in solar cells [20].

The aim of this work is to present a study of the sol-gel obtained ZnO-TiO_2 films. Recently, we studied sol-gel TiO_2 films doped with vanadium, manganese oxide and zirconium oxide in respect to its structural and optical properties [21,22]. The films were deposited by dip-coating method on Si and glass substrates. We had some research on sol-gel preparation and investigation of ZnO films [23]. The films, subject of this study were spin-coated on silicon and glass substrates. Their structure and crystal evolution was examined by XRD and FTIR analysis. Optical characterization was performed by UV-V1S-N1R spectroscopy. The effect of the annealing treatments on the ZnO-TiO_2 film properties was investigated compared with the single oxide films (ZnO and TiO_2).

2. EXPERIMENTAL DETAILS

The zinc and titanium precursor solutions were prepared separately. The zinc precursor solution was obtained by dissolving zinc acetate dehydrate in an absolute ethanol. Triethanolamine (TEA) was used as a complexing agent and the molar ratio TEA/Zn was fixed to 1. Then, the solution was mixed at 50 °C/1 h by stirring with a magnetic stirrer at atmospheric pressure and ultrasonically treated at 40 °C/30 min. The obtained sol was transparent and stable for six months.

The precursor for titanium oxide film forming solution was titanium ethoxide. The introduction of glacial acetic acid (Fluka type) caused acetate modification, which was an exothermic reaction. Furthermore, the solution was modified by a small amount of water, leading to hydrolysis and condensation reactions, which resulted in a transparent gel. A small amount of acetylacetone acted as a peptizing agent and stabilizer. The solution became transparent after aging 1 week. More details about titanium sol formation can be found in [24]. These solutions were used for deposition of pure ZnO and TiO_2 films.

For the preparation of the mixed oxide films, the two sols were mixed in molar ratio 1:1. The thin films were deposited by the spin-coating procedure at 4000 rpm, followed by a low temperature firing at 400 °C/30 min in air. In order to increase the film thickness, the layer deposition was repeated five times. ZnO, TiO_2 and ZnO-TiO_2 films on Si wafers were annealed at 400, 500, 600 and 750 °C for 1 h in air. In the case of the glass substrates, the annealing temperature was limited to 600 °C.

The film thickness for ZnO films are in the range of 130-100 nm depending on the annealing temperature, the corresponding values for TiO_2 films are 100-80 nm. The mixed ZnO-TiO_2 films are 60-80 nm thick.

XRD spectra of sol-gel thin films were recorded by means of XRD diffractometer Bruker D8, at the grazing angle 2° and step time 8 s and step 0.1°. FTIR measurements were performed in the spectral region 350-1600 cm^{-1} by Shimadzu FTIR Spectrophotometer IRPrestige-21.

Optical measurements were done with the help of UV-3600 Shimadzu spectrophotometer. The thin films for optical characterization were obtained on glass substrates, followed by annealing at the temperatures of 400, 500 and 600 °C.

3. RESULTS

3.1. XRD study

The structural changes, provoked by the thermal treatments at different temperatures, were studied by XRD technique. Fig. 1 shows the recorded spectra of ZnO and ZnO-TiO films. The spectrum of ZnO-TiO_2 films annealed at 400 °C reveals a high degree of an amorphous phase as can be assumed from the shapes and the intensities of the XRD lines. A broad band located at 34.9° and a weak shoulder at 56.5° are assigned to the hexagonal ZnO (002) and (110) (JCPDS 01-07-8070). The strong peak located at $2\theta = 55.2°$ is probably due to anatase TiO_2 (JCPDS 00-021-1272). This peak is intense and might be a sign of some preferential growth of TiO_2 in 211 direction. On the other hand, the spectrum of ZnO film, annealed at 400 °C reveals five well defined XRD maxima, indicating polycrystalline structure. These peaks correspond to hexagonal wurtzite phase [23].

More complicated features are observed in the spectrum of the mixed oxide system, treated at 500 °C (Fig. 1(b)). The reflections, due to hexagonal ZnO crystal phase, vanished. The spectrum form suggests a high degree of amorphous fraction. The broad band at 29.6° and the clearly seen maximum at 34.9° are assigned to Zn_2TiO_4 (cubic symmetry; JCPDS 00-025-1164). The other two peaks at 38.3 and 55.1° can be referred to anatase TiO_2. The peak located at 54.2°, which is most probably related to cubic ZnO_2 for the XRD line at the same position, appeared in the spectrum of ZnO film, annealed at 600 °C (see Fig. 1(c)). It must be noted that anatase TiO_2 also expressed maximum at this location.

The annealing at 600 °C (Fig. 1(c)) induces crystallization and several new intense peaks are detected. The XRD lines at 29.8 and 35.17° correspond either to Zn_2TiO_4, or to $ZnTi_{1.5}O_4$ (JCPDS 04-006-5709). The fraction of Zn_2TiO_4 phase is manifested by other strong reflections at 42.58, 43.12 and 53.33° [25]. Anatase phase of titanium oxide can also be observed at 38.18° as well as the reflection at 54.5°, which can be associated both to cubic ZnO_2 or anatase TiO_2. The broad band at 56° is related to the presence of hexagonal ZnO phase. The peak broadness indicates a certain presence of amorphous phase.

Fig. 1. *XRD spectra of the sol-gel ZnO-TiO_2 and ZnO films, treated at different temperatures.*

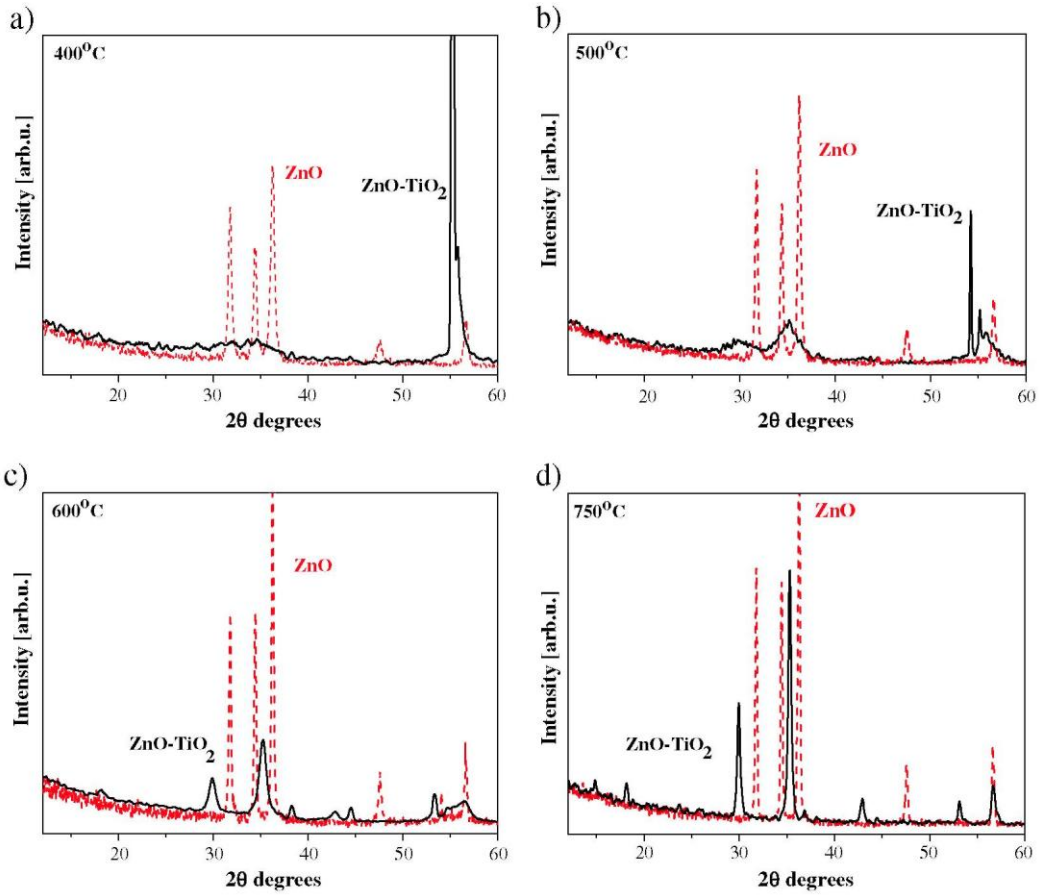

The increase of the annealing temperature to 750 °C leads to better expressed crystallization. The three intense lines (29.9°, 35.32°, 53.04°) correspond to Zn_2TiO_4, including the strongest XRD peak at 35.32° (Fig. 1(d)). The two weaker reflections at 17.99 and 23.69° might be assigned to $ZnTiO_2$ cubic phase (JCPDS card 00-39-0190). The hexagonal ZnO phase is presented by a weak reflection at 42.97° and a strong peak at 56.6°.

The average crystallite sizes were estimated from XRD data according to Scherrer's formula and the results are presented in Table 1. It is seen that the crystallite sizes are sensitive to the annealing procedures.

3.2. Vibrational properties

FTIR study was performed to reveal the changes in the vibrational properties upon heat treatments for the studied ZnO-TiO_2 thin films. The spectra are presented in Fig. 2 and the FTIR data is summarized in Table 2. FTIR analysis of pure sol-gel ZnO films has been previously reported [23]. The infrared spectra of ZnO films, treated at 400, 500 and 600 °C showed that the main absorption band (very strong) is located near 395 cm^{-1} and after the highest temperature annealing it slightly shifted to 403 cm^{-1}. This band is due to the stretching vibrations of Zn-O bonds [26]. The other weaker bands at 425, 470 cm^{-1} are also attributed to the stretching vibrations of ZnO. The absorption line, which had appeared at 515 cm^{-1} only in the spectrum of ZnO film, treated at 750 °C, is one of the infrared active modes (408 and 513 cm^{-1}) that are theoretically confirmed. This line corresponds to wurtzite zinc oxide [27].

The bands in the spectral range from 1200 cm^{-1} up to 4000 cm^{-1} are attributed to the vibrations of the organic residuals and to water incorporation. The mixed ZnO-TiO_2 films show absorption bands in 3600-3200 cm^{-1} connected to the stretching vibrations of hydroxyl groups. The 3450 cm^{-1} band arises from the superposition of the OH groups and the symmetric and asymmetric OH modes of molecular water coordinated to Ti^{4+} cations [28]. The 3650 and 3780 cm^{-1} (observed in the FTIR spectra of samples, annealed at 400, 500 and 600 °C) are assigned to the physically absorbed water. It is interesting to note that some vibrations of the hydroxyl groups can be still detected even after the highest temperature treatment. The peaks around 2908 cm^{-1} are due to the existence of symmetric and asymmetric C-H bonds, the C = O stretching vibrations are expressed at 1729 and 1568 cm^{-1} [28].

The IR spectra manifest absorption bands in the region 350-1200 cm^{-1}, which are due to the oxygen-metal linkages. ZnO-TiO_2 thin films annealed at 400 and 500 °C show only weak absorption bands in this spectral range. More intense bands can be observed in the spectra of the samples that had undergone higher temperature annealing. The 1R spectrum of 400 °C annealed films shows several peaks attributed to Zn-O bonds. The clear feature at 416 cm^{-1} is assigned to wurtzite ZnO. The weak band at 435 cm^{-1} can be due to the Ti-O stretching vibrations of anatase TiO_2 [29]. The clear band at 629 cm^{-1} is associated to the vibrations of TiO6 polyhedron.

When the annealing temperature is increased to 500 °C, the FTIR analysis reveals the presence of the same absorption bands. The IR band at 419 cm^{-1} became stronger (due to either Ti=O or to wurtzite ZnO [30]). The new weak peak located at 511 cm^{-1} is attributed to crystalline wurtzite zinc oxide. The weak bands, attributed to anatase TiO_2 are also detected. A broad absorption at 1040 cm^{-1} is due to Si-O-Si symmetrical stretching vibration due to the silicon substrate and its intensity increases with higher temperatures.

The annealing at 600 °C leads to the manifestation of two new bands at 709 and 728 cm^{-1}, which are connected to Zn-O bonds [31]. The peaks at 417 and 513 cm^{-1} are a sign of the presence of wurtzite ZnO. TiO_2 fraction is manifested by two features at 544 cm^{-1} (stretching vibrations of Ti-O-Ti group) and at 625 cm^{-1} (vibrations of TiO_6 polyhedron) [32]. Meanwhile, the IR feature at 544 cm^{-1} also corresponds to the presence of Ti06 group existing in the phases of Zn_2TiO_4 and $ZnTiO_3$ [25].

The ZnO-TiO_2 film treated at 750 °C reveals a peak at 421 cm^{-1}, which is a sign of wurtzite ZnO as well as other absorption bands related to Zn-O bonds. At the same time, the absorption maxima at 839 and 874 cm^{-1} can be attributed to vibrations of anatase and amorphous TiO_2, respectively [32].

3.3. Optical characterization

The optical properties of ZnO-TiO_2 films were compared with those of the single component films (ZnO and TiO_2), obtained from the respective sols. As can be seen from Fig. 3, all three types of the sol-gel films manifest a high transmittance in the visible and near-infrared spectral range after being annealed at 600 °C/1 h.

It must be noted that the transmittance is measured by using an integrating sphere in the spectral range 240-2600 nm, therefore the transmittance is total (including direct and diffusive transmittance). The pure ZnO films manifest 90.6% for wavelengths above 1400 nm, TiO_2 films show 76%. The mixed Zn/Ti oxide films are 85% transparent in the visible and near IR spectral region.

Table 1: *XRD data for sol-gel ZnO-TiO_2 films, treated at different temperatures.*

Material	Annealing	Crystal Phase	XRD peak	Size
TiO_2-ZnO	600 °C	Zn_2TiO_4	29.8	16.4 nm
			35.17	14.8 nm
		TiO_2	38.18	29.8 nm
TiO_2-ZnO	750 °C	Zn_2TiO_4	29.9	30.7 nm
			35.32	34.2 nm
		ZnO	56.6	26.3 nm
ZnO	600 °C		average	35 nm
	750 °C			40 nm

***Fig. 2.**: FTIR spectra of the sol-gel ZnO-TiO_2 films, annealed at 400, 500, 600 and 750 °C (a) and compared with FTIR spectra of ZnO films (b).*

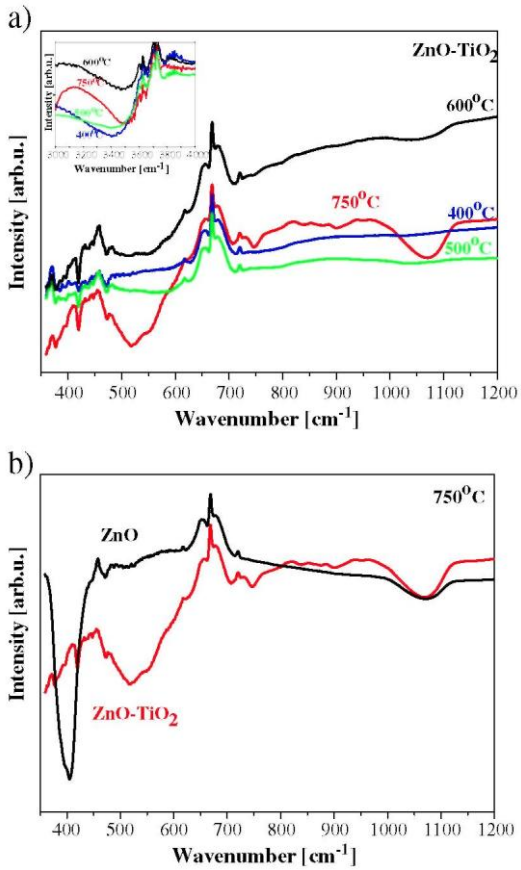

***Fig. 3.** Transmittance spectra of sol-gel films of ZnO, TiO_2 and ZnO-TiO_2, annealed at 600 °C.*

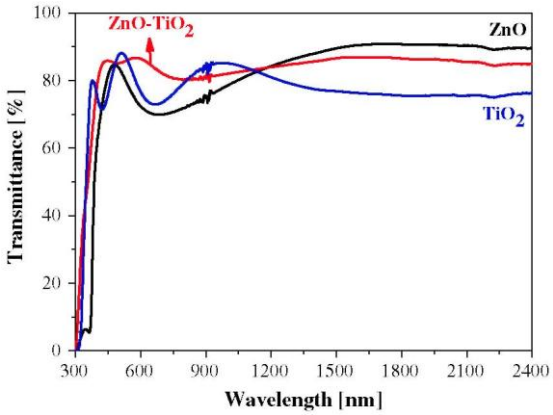

Table 2: *FTIR data for sol-gel ZnO-TiO_2 films, treated at different temperatures.*

Annealed at 400 °C/1 h	**Annealed at 500 °C/1 h**	**Annealed at 600 °C/1 h**	**Annealed at 750 °C/1 h**	**Assigned to**
		378.1 cl	374.2W	
385.6 cl				Zn—O bonds
395.1 cl	393.3 cl			Zn—O bonds
416.1	419.9 st	417.9 cl	421.7 cl	ν_s(Zn—O), Wurtzite phase
435.1 w	435 weak			ν_s(Ti-O), anatase
452.2 w	448			Zn-O or TiO_2 anatase
473.2 cl	473.2 cl	473.2 cl	473.2 cl	Zn-O
	511.2 w	513.2 br, cl 543.5 br, cl	520.6 br, str	Characteristic for wurtzite ZnO ν_s(Ti-O-Ti)
629.1 cl	627.3 cl	625.3 sh	623.4 sh	Vibrations of TiO6 polyhedron
	710.9 cl	709.1 cl	707.2 cl 747.1 cl 838.5 cl 874.6 cl 901.2 cl	Zn-O vibrations Zn-O vibrations Anatase TiO_2 Amorphous TiO_2
	1040.1 br	1043.9 cl br	1068.7 str 1266.2 cl	Si-O-Si vibrations ν_s(COO)
	1427.4 cl		1447.6 cl	CH_2 bending vibrations
1583.1 cl	1568.5 cl	1568.5 w		ν_s(C = O)
		1729.8 w	1739.6 cl, br	C = O monomer stretching vibrations
		2908.0 w	2908 cl, br	ν_s (CH or CH_2) ass.
3452.6 br	3482.1 br	3451.9 broad	3522.5 br, cl	Hydroxyl group
3655.4 cl	3653.2 cl	3673.4 w		vibrations of physically absorbed water
3784.9 w	3777.1 cl	3774.1 w		Non-hydrogen bonded OH groups (free OH groups).

Table 3: *Optical band gap values determined from spectrophotometric measurements.*

Material	Annealing temperature	E_g [eV]	Refractive index
ZnO	400 °C	3.29	2.32
	500 °C	3.28	2.33
	600 °C	3.27	2.33
ZnO-TiO_2	400 °C	3.88	2.19
	500 °C	3.91	2.18
	600 °C	3.89	2.19
TiO_2	400 °C	3.74	2.22
	500 °C	3.73	2.22
	600 °C	3.70	2.23

Fig. 4. *UV-VIS spectra of sol-gel TiO_2 (a) and ZnO-TiO_2 (b) films, annealed at different temperatures.*

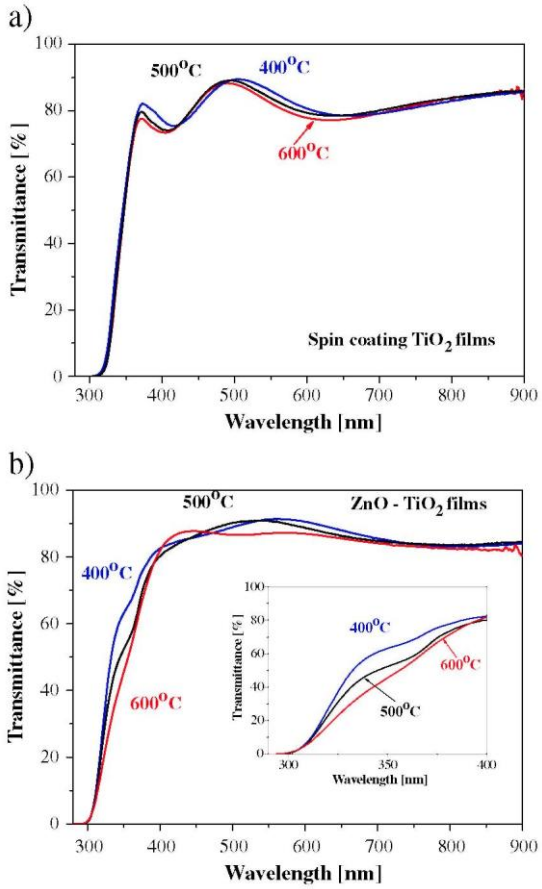

Fig. 4 presents the influence of the thermal treatments on the optical properties for TiO_2 and ZnO-TiO_2 films. Optical properties of spin-coated ZnO films have been previously reported [23]. The transparency of ZnO films is significantly affected by the annealing temperature. The increase of the annealing temperature diminishes the transmittance values from 91% to 80% (at λ = 550nm). The excitonic absorption feature of the ZnO films is revealed by the small shoulders appearing at~322, 321 and 320 nm (after annealing at 400, 500, 600 °C, respectively). The excitonic absorption of bulk ZnO is located at ~373 nm [33]. These shifts can be attributed to some size effect and/or the film morphology [34]. On the other hand, exciton absorption is also a sensitive indicator of material quality and crystal structure, the existence of which is usually associated with a low density of defects and little strain [35].

TiO_2 films show a slight decrease of the transparency due to the annealing procedures and the transmittance changes from 86.5% to 82% (at λ = 550nm) for the films, treated at 400 and 600 °C, respectively. The transmittance decrease of the sol-gel TiO_2 films with the increase in the annealing temperature might be related to the increase of scattering loss owing to crystallization [36].

Similar optical behaviour is observed for ZnO-TiO_2 films (see Fig. 4b). The change of the transparency is from 92% (at λ. = 550 nm with the annealing temperature at 400 °C) up to 87% (after annealing at 600 °C). The spectra of ZnO-TiO_2 films also presented some excitonic absorption features depending on the annealing temperature. No excitonic absorption can be distinguished for the sample, annealed at the highest annealing temperature (600 °C). On the other hand, the ZnO-TiO_2 films, treated at 400 and 500 °C show absorption peaks at 363 and 362 nm, respectively. They are considerably altered in comparison with pure zinc oxide films and much closer to those of bulk ZnO.

The optical band gap (E_g) can be estimated from transmittance measurements considering direct gap semiconductors. The optical band gap values of ZnO films, determined by second derivative spectrum [27], are 3.29 eV, 3.28 and 3.27 eV for the samples, annealed at 400 °C, 500 °C and 600 °C, respectively. The effect of

annealing procedures is almost negligible. The E_g value of bulk ZnO is 3.3 eV [37]. The small decrease in the band gap values after heat treatment for the ZnO films might be attributed to the quantum confinement of the charge carriers in very fine nanocrystalline grains [38]. The estimated optical band gaps of TiO_2 films are 3.74 eV (400 °C); 3.73 eV (500 °C) and 3.70 eV (600 °C) with a slight decrease after increasing the annealing temperature. These results are in agreement with literature data for TiO_2 films, where the Eg varies between 3.6 and 4 eV [39,40].

The bulk anatase TiO_2 possesses an optical band gap of about 3.2 eV. The large difference with the obtained results might be due to the different crystalline state (polycrystalline structure), grain sizes and crystalline structure of the thin films and bulk material [39,41]. The E_g values of the mixed films are in the range of 3.88 and 3.91 eV as can be seen in Table 3.

4. DISCUSSION

The XRD study points out that the sol-gel ZnO films crystallize at the low annealing temperature of 400 °C. The high degree of crystallization is manifested with the well defined main peaks (five XRD lines appeared in all spectra). Their intensity is significantly enhanced by increasing the annealing temperatures. On the other hand, XRD study of the mixed ZnO-TiO_2 films shows more complicated polycrystalline structures. The presence of many crystal phases corresponding to pure oxides or titanates is detected. The amorphous phase is also presented especially for the ZnO-TiO_2 films annealed at 400 and 500 °C, where it is dominant. The high temperature annealings at 600 and 750 °C induce more pronounced crystallization with several intense reflections, but the presence of the amorphous phase can still be detected as well. TiO_2 anatase phase is revealed in the films, treated at 400, 500 and 600 °C. The corresponding XRD lines significantly weaken with the increase in the annealing temperatures. At the highest annealing temperature of 750 °C, no titanium oxide crystal phase is observed. The XRD data suggests that Zn_2TiO_4 becomes a favored phase as the annealing temperature is increased to 750 °C. It can also be proposed that the increase of the duration of the post heat treatment at this temperature can induce crystallization of a single phase material such as Zn_2TiO_4.

The annealing procedures lead to the formation of bigger crystallites. The grain size values for Zn_2TiO_4 phase increased from 16.4 nm (600 °C annealing) up to 30.7 nm after the high temperature treatment at 750 °C. The same tendency is observed in ZnO films, where the crystallite sizes varied when the annealing temperature was increased from 22 nm (400 °C) to 40 nm (750 °C).

FT1R results are in a good agreement with the XRD characterization, which reveals that a certain amorphous phase is still remaining even after the highest temperature treatment. XRD data showed no presence of anatase titanium dioxide in the film structure of the 750 °C annealed film as the FTIR analysis revealed. It is well known that the FT1R technique is very sensitive to the existence of small crystalline phases. XRD study points out that after the highest temperature annealing, the predominant crystal phase is Zn_2TiO_4.

IR bands related to (TiO6), [ZnO4] and (ZnO6) are expected if Zn_2TiO_4 is present [42]. The absorption range of condensed [TiO6] octahedral groups occurs at 650-550 cm^{-1}, and the absorption range of isolated (ZnO4) tetrahedral groups occurs at 500-400 cm^{-1} [42].As can be seen in Fig. 2 and Table 2, several absorption lines are located in these spectral regions, which supports the results from the XRD measurements.

The results from the optical characterization for ZnO-TiO_2 films are very interesting. There is no significant dependence on the annealing temperatures on their transparency. On the other hand, the optical band gaps of the mixed system are higher than those of the pure metal oxides. The E_g values are in the range of 3.88 and 3.91 eV as can be seen in Table 3. The studied sol-gel ZnO-TiO_2 films possess in their structure mixtures of phases, including wurtzite ZnO, anatase TiO_2, Zn_2TiO_4 and amorphous fraction after annealing at 400, 500 and 600 °C. Similar results for the optical band gaps of mixed ZnO-TiO_2 materials are reported by other authors [43], and they had estimated E_g, varying from 3.84 up to 4.12 eV in proportion to the TiO_2 content. On the other hand, Zn_2TiO_4 films are reported to have E_g = 3.7 eV [44], The refractive indexes of the spin coated TiO_2, ZnO and mixed Zn/Ti oxide films can be calculated using the equation given in ref. [45]. The corresponding results are also presented in Table 3. The refractive index for TiO_2 films is 2.22, which is close to the literature values [46]. The refractive index of sol-gel ZnO films is about 2.32, which corresponds to polycrystalline ZnO and is in an agreement with previous reported results [45]. The mixed Zn/Ti oxide films reveal the values of the refractive index (2.18 and 2.19) smaller then those of pure oxide films.

5. CONCLUSIONS

Thin films of ZnO-TiO_2 have been successfully deposited by the sol-gel method and spin-coated on silicon and glass substrates. Their structural and vibrational properties have been studied as a function of the annealing temperatures (400-750 °C). XRD analysis shows that the structure of the sol-gel ZnO-TiO_2 films is a mixture of crystalline phases and amorphous fraction. The highest temperature annealing results in polycrystalline films with the predominant fraction of Zn_2TiO_4. The optical properties of ZnO-TiO_2 films are compared with those of single component films (ZnO and TiO_2). The mixed oxide films present high transmittance with a slight decrease with an increase in the annealing temperature. Their optical transparency reaches 92% over the visible range. The sol-gel mixed films based on ZnO and TiO_2 can be applicable in developing materials for optoelectronic devices.

References

[1] Y.Q. Fu, J.K. Luo, X.Y. Du, A.J. Flewitt, Y. Li, G.H. Markx, A.J. Walton, W.I. Milne, Sens. Actuators, B 143 (2010) 606.
[2] S. Lee, E. Shim, H. Kang, S. Pang, J. Kang, Thin Solid Films 473 (2005) 31.
[3] W.Y. Weng, T.J. Hsueh, S.J. Chang, S.P. Chang, C.L. Hsu, Superlattices Microstruct. 46 (2009) 797.
[4] M.W. Ann, K.S. Park, J.H. Heo, D.W. Kim, K.J. Choi, J.G. Park, Sens. Actuators, B 138 (2009) 168.
[5] S.B. Ambade, R.S. Mane, A.V. Ghule, M.G. Takwale, A. Abhyankar, B. Cho, S. Han, Scripta Mater. 61 (2009) 12.
[6] K.J. Chen, F.Y. Hung, S.J. Chang, S.J. Young, J. Alloy. Comp. 479 (2009) 674.
[7] Z. Seeley, Y.J. Choi, S. Bose, Sens. Actuators, B 140 (2009) 98.
[8] G. San Vicente, A. Morales, M.T. Gutierrez, Thin Solid Films 391 (2001) 133.
[9] C. Wang, S. Lin, Y. Chen, J. Phys. Chem. Solids 69 (2008) 451.
[10] R. Dholam, N. Patel, M. Adami, A. Miotello, Int J. Hydrogen Energy 34 (2009) 5337.
[11] N. Bouhssiraa, M.S. Aida, A. Mosbaha,J. Cellier, J. Cryst Growth 312 (2010) 3282.
[12] T. Iida, Y. Takamido, T. Kunii, S. Ogawa, K. Mizuno, T. Narita, N. Yoshida, T. Itoh, S. Nonomura, Thin Solid Films 516 (2008) 807.
[13] O. Lupana, T. Pauporté, L Chow, B. Vianae, F. Pelle, L.K. Ono, B. Roldan Cuenya, H. Heinrich, Appl. Surf. Sci. 256 (2010) 1895.
[14] S. Ilican, Y Caglar, M. Caglar, F. Yakuphanoglu, Appl. Surf. Sci. 255 (2008) 2353.
[15] Zh. Liu, Ch. Liu, J. Ya,E. Lei, Renewable Energy 36 (2011) 1177.
[16] R. Reisfeld, Opt. Mater. 16 (2001) 1.
[17] Y. Guim, Sh. Li, Ch. Li, Microelectron. J. 39 (2008) 1120.
[18] M. Zhang, T. An, X. Liu, X. Hu, G. Sheng, J. Fu, Mater. Lett. 64 (2010) 1883.
[19] D.W. Kim, S. Lee, H.S. Jung, J. Kim, H. Shin, K.S. Hong, Inter. J. Hydrogen Energy 32 (2007) 3137.
[20] M.R. Vaezi, J. Mater. Process. Techn. 205 (2008) 332.
[21] T. Ivanova, A. Harizanova, M. Surtchev, Z. Nenova, Sol. Energy Mater. Sol. Cells 76 (2003) 591.
[22] T. Ivanova, A. Harizanova, T. Koutzarova, N. Krins, B. Vertruyen, Mater. Sci. Eng. B 165 (2009) 212.
[23] T. Ivanova, A. Harizanova, T. Koutzarova, B. Vertruyen, Mater. Lett 64 (2010) 1147.
[24] O. Harizanov, Harizanova, Sol. Energy Mater. Sol. Cells 63 (2000) 185.
[25] M.R. Mohammadi, D.J. Fray, J. Eur. Ceram. Soc. 30 (2010) 947.
[26] Y.L Liu, Y.C Liu, Y. Liu, D. Shen, Y. Lu, J.Y. Zhang, X.W. Fan, Phys. B 322 (2002) 31.
[27] D. Djouadi, A. Chelouche, A. Aksas, M. Sebais, Phys. Procedia 2 (2009) 701.
[28] L. Y. Zhu, G. Yu, X.Q. Wang, D. Hu, J. Colloid Interface Sci. 336 (2009) 438.
[29] N. Sijakovic-Vujicicic, M. Gotić, S. Musić, M. Ivanda, S. Popović, J. Sol Gel Sci. Techn. 30 (2004) 5.
[30] M. Zerdali, S. Hamzaoui, F.H. Teherani, D. Rogers, Mater. Lett 60 (2004) 504
[31] R. Hong, T. Pan, J. Qian, H. Li, Chem. Eng. J. 119 (2006) 71.
[32] A. Verma, M. Kar, S.A. Agnihotry. Sol. Energy Mater. Sol. Cells 91 (2007) 1305.
[33] R Shinde, T.P. Gujar, C.D. Lokhande, Sol. Energy Mater. Sol. Cells 91 (2007) 1055.
[34] Z.-X. Yang, X. Du, W. Zhong, Y.-X. Yin, M.-H. Xu, Ch. Au, Y.-W. Du, J. Alloy. Comp. 509 (2011)3403.
[35] Z.G. Yao, X.Q. Zhang, H.K. Shang, X.Y. Teng, Y.S. Wang, S.H. Huang, Chin. Phys. 14 (2005) 1205.
[36] B. Zhao, J. Zhou, Y. Chen, Y. Peng, J. Alloy. Comp. 509 (2011) 4060.
[37] R. Prez-Casero, A. Gutírrez-Llorente, O. Pons-YMoll, W. Seiler, R. Defourneau, D. Defourneau, E. Millon, J. Perrire, P. Goldner, B. Viana, J. Appl. Phys. 97 (2005)1.
[38] A.E. Jimenez-Gonzeilaz, P.K. Nair, Semicond. Sci. Technol. 10 (1995) 1277.
[39] J.M. Gonza'lez-Leal, R. Prieto-Alcon, J.A. Angel, E. Marquez, J. Non-Cryst Solids 315 (2003) 134.
[40] C. Quiñonez, W. Vallejo, G. Gordillo, Appl. Surf. Sci. 256 (2010) 4065.
[41] Y. Sheng, L. Liang, Y. Xu, D. Wu, Y. Sun, Opt. Mater. 30 (2008) 1310.
[42] A.C. Chaves, S.J.G. Lima, R.C.M.U. Araújo, M.A.M.A. Maurera, E. Longo, P.S. Pizani, L.G.P. Simões, L.E.B. Soledade, A.G. Souza, I.M.G. Santos, J. Solid State Chem. 179 (2006) 985.
[43] L. Irimpan, B. Krishnan, V.P.N. Nampoori, P. Radrakrishnan, J. Colloid Interface Sci. 324 (2008) 99.
[44] SA Mayen-Hernandez, G. Torres-Delgado, R. Castanedo-Perez, J. Marquez Marin, M. Gutierrez-Villarreal, O. Zelaya-Angel, Sol. Energy Mat Sol. Cells 91 (2007) 1454.
[45] N. Ekem, S. Korkmaz, S. Pat, M.Z. Balbag, E.N. Cetin, M. Ozmumcu, Int J. Hydrogen Energy 34 (2009) 5218.
[46] H. Yang, H. Fan, Y. Xi, J. Chen, Zh. Liet, Appl. Surf. Sci. 254 (2008) 2685.